



Electromagnetic Energy Resolution Studies with the ATLAS Detector

Cristina-Andreea Alexe, The University of Manchester, United Kingdom

Supervisors: Ludovica Aperio Bella, Filip Nechanský, Craig Wells

September 7, 2022

Abstract

The relative energy resolution of electrons detected in the Liquid Argon (LAr) Calorimeter at ATLAS receives a contribution from the sampling term a . A method to determine an effective sampling term is presented, using 350 pb^{-1} of low energy, low pile-up data $\langle \mu \rangle = 2$ collected by ATLAS at $\sqrt{s} = 13 \text{ TeV}$ between 2017 and 2018. By comparing the J/ψ mass resonance peak position between data and Monte Carlo simulation, the energy scale correction is extracted per region in pseudorapidity. The presented results translate into an improved modelling of the response of the LAr Calorimeter, beneficial to the various measurements and searches carried out with the ATLAS detector.

Contents

1	Introduction	3
2	Electron detection at ATLAS	4
2.1	The Liquid Argon Electromagnetic Calorimeter	4
2.2	Relative energy resolution	4
3	Determination of the effective sampling term a	5
3.1	Introduction to the measurement	5
3.2	Measurement of energy scale and resolution corrections	5
3.3	Preparation of the data	7
3.3.1	Initial preparation	7
3.3.2	Separation of prompt and non-prompt J/ψ	7
3.4	Monte Carlo samples	8
3.5	Fit of the data	8
3.6	Data and Monte Carlo fit	10
4	Results	10
5	Conclusion and discussion	12

1 Introduction

Electron detection is an essential stage for the numerous measurements and searches exploring the electroweak sector that are performed at the ATLAS experiment. An accurate determination of the electron energy resolution is thus required, particularly for precision measurements of the Standard Model parameters, such as the mass of the W boson or particle decay cross-sections.

At ATLAS, electrons are detected in the Liquid Argon (LAr) Electromagnetic Calorimeter, where they produce an electromagnetic (EM) shower. The relative energy resolution receives a contribution from the sampling term a , due to the stochastic behaviour of shower development in the detector. The resolution is also dependent on pile-up¹ noise and, at high energies especially, on detector imperfections such as radiation damage.

The purpose of this project is to obtain an effective sampling term a by removing the remaining contributions to the total resolution as much as possible. This is achieved by studying the J/ψ resonance curve with the decay $J/\psi \rightarrow e^+e^-$, representing a low energy regime, with 350 pb⁻¹ of low pile-up data, quantified¹ by $\langle\mu\rangle = 2$, collected by ATLAS at $\sqrt{s} = 13$ TeV between 2017 and 2018.

Comparing the reconstructed J/ψ peak position and width in data and the Monte Carlo (MC) simulation allows for the energy calibration and the determination of the energy resolution correction, respectively. The sampling term depends significantly on pseudorapidity η , so the analysis of the data is split into regions of η using the following binning $\pm[0.0, 0.4, 0.8, 1.37 - 1.52, 2.47]$.

In order to fit the J/ψ peak in the data, its shape must be first obtained from the MC simulation to ease the estimation of background. Due to delays in the production of the MC, an alternative method for estimating the background from data alone was developed.

The results presented in this report include the values of the energy scale correction per regions of pseudorapidity. Due to time considerations, only the method of determining the energy resolution corrections was presented, although its implementation in the existing framework is straightforward.

The presented improvement in the determination of electron energy resolution at the LAr Calorimeter is useful for the various precision measurements and searches performed with the ATLAS detector.

¹Pile-up is the average number of particle interactions per bunch-crossing and $\langle\mu\rangle$ represents the mean number of additional inelastic proton-proton collisions in the same bunch-crossing.

2 Electron detection at ATLAS

2.1 The Liquid Argon Electromagnetic Calorimeter

The ATLAS detector is a general-purpose particle physics detector at the Large Hadron Collider, with coverage in solid angle of approximately 4π . Electrons and photons produced in proton-proton collisions are detected in ATLAS with the Liquid Argon Electromagnetic Calorimeter. This is located with respect to the proton beam pipe between the Inner Tracker and the Hadronic Calorimeter. The LAr Calorimeter is a sampling calorimeter and has an accordion geometry. Before the accordion calorimeter, a presampler is added to correct for energy loss upstream the calorimeter [1].

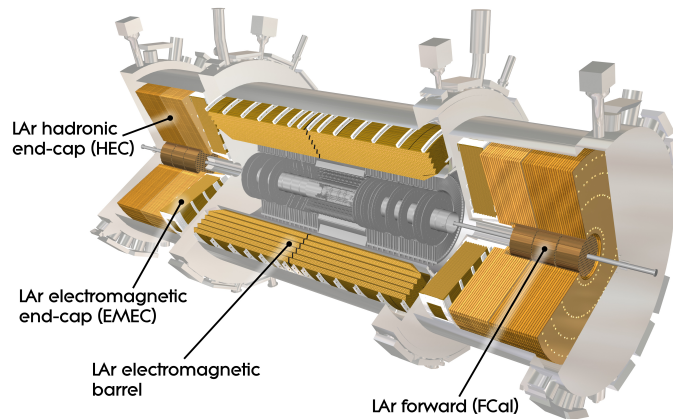


Figure 1: Schematic representation of the ATLAS Liquid Argon Calorimeter, made of a barrel section and two endcap sections [2].

In order to define kinematic parameters such as pseudorapidity η , the coordinate system used at ATLAS is defined as such: the origin is at the centre of the detector, with the x-axis pointing to the centre of the LHC ring, the y-axis pointing upwards and the z-axis along the beam pipe. In cylindrical coordinates, ϕ is the azimuthal angle about the z-axis and θ is the polar angle in the y-z plane.

2.2 Relative energy resolution

The relative energy resolution for electrons and photons is given by:

$$\frac{\sigma_E}{E} = \frac{a}{\sqrt{E}} \oplus \frac{b}{E} \oplus c, \quad (1)$$

where the symbol \oplus represents addition in quadrature and the three terms are:

- a , the sampling term. This term results from the stochastic evolution of EM showers in the detector. Due to the dependence on particle energy, the sampling term is dominant at low energies. The design value for a at the ATLAS LAr Calorimeter is 10% [3];
- b , the noise term. This term receives contribution from both electronic and pile-up noise;
- c , the constant term. At large energies, the total relative resolution approaches the constant term, which does not depend on the particle properties but on detector imperfections such as radiation damage or imperfections in geometry. The design value for c at the ATLAS LAr Calorimeter is 0.7% [3].

The parameters a , b and c are all dependent on the amount of material in the detector that the particle interacts with, quantised by the pseudorapidity η , defined in terms of the polar angle θ as:

$$\eta \equiv -\ln \left[\tan \left(\frac{\theta}{2} \right) \right]. \quad (2)$$

Due to the strong dependence on pseudorapidity of the terms in formula (1), the analysis is performed for electrons sorted by η , using the following binning: $\pm[0.0, 0.4, 0.8, 1.37 - 1.52, 2.47]$.

3 Determination of the effective sampling term a

3.1 Introduction to the measurement

Usually, the total resolution is constrained at given η and mean electron energy ~ 40 GeV using the Z boson resonance width [4]. This regime gives an effective constant term c , to be added in quadrature to the expected resolution. In this report, an effective sampling term a is obtained by constraining the total resolution at given η and for average electron transverse energy of ~ 11 GeV by studying the J/ψ resonance width.

In order to isolate the a term from the contributions from the pile-up and constant terms, the analysis is performed in a low-pile up, low energy regime. The J/ψ resonance curve is studied with 350 pb^{-1} of data with $\langle \mu \rangle = 2$ collected by ATLAS at $\sqrt{s} = 13$ TeV between 2017 and 2018.

3.2 Measurement of energy scale and resolution corrections

Similarly to how the decay $Z \rightarrow e^+e^-$ is a standard calibration channel for electron energy measurements [4], in the low transverse momentum regime $J/\psi \rightarrow e^+e^-$ represents an additional "standard candle" for electron energy calibration. The invariant mass of the dielectron system is given by:

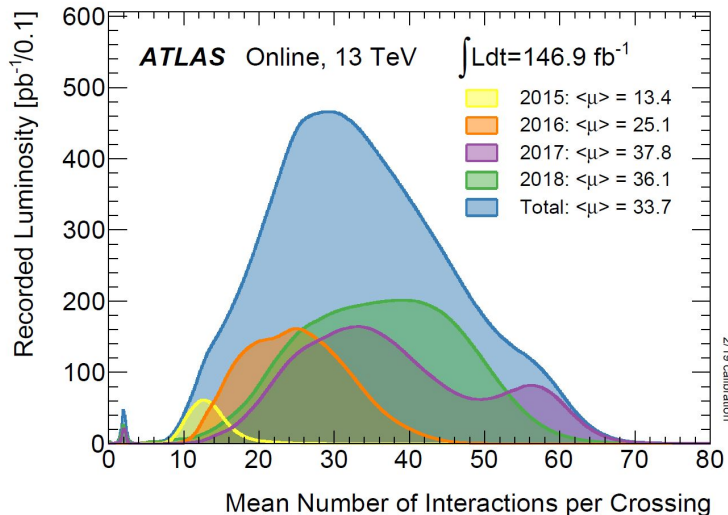


Figure 2: Profile of the pile-up produced at ATLAS between 2015 and 2018 [5].

$$m_{ee}^2 = 2E_1E_2(1 - \cos \theta_{12}), \quad (3)$$

where E_1 , E_2 denote individual electron energies and θ_{12} is the angle between the electrons. The energy scale correction α is defined as the difference between the reconstructed electron energy in data and the Monte Carlo simulated sample:

$$E_{Data}(\eta) = E_{MC}(\eta)(1 + \alpha(\eta)). \quad (4)$$

The disagreement between data and MC due to the energy scale correction propagates through formula (3) to disagreement between the reconstructed dielectron invariant mass in data and MC:

$$m_{ee}^{Data} = m_{ee}^{MC} \left(1 + \frac{\alpha_i + \alpha_j}{2}\right), \quad (5)$$

where the indices (i, j) denote the η bin in which a given electron is found. Thus, comparing the reconstructed J/ψ mass peak position in data and MC allows for the determination of the energy scale correction α per pseudorapidity bin.

Similarly, the residual resolution corrections of the sampling term a can be defined from the difference in relative energy resolution in data and MC, assuming the constant and noise terms to be negligible due to the low energy and low pile-up regimes, respectively:

$$\left(\frac{\sigma}{E}\right)_{Data} = \left(\frac{\sigma}{E}\right)_{MC} \oplus \frac{\Delta a}{\sqrt{E}}. \quad (6)$$

Thus, after the scale correction is determined, a comparison of the reconstructed J/ψ mass peak width gives the resolution correction in bins of η :

$$\sigma_{m_{ee}^{Data}} = \left(1 + \frac{\alpha_i + \alpha_j}{2}\right) \sqrt{\sigma_{m_{ee}^{MC}}^2 + \frac{m_{ee}^2 MC}{4} \left(\frac{\Delta a_i^2}{\langle E_i \rangle} + \frac{\Delta a_j^2}{\langle E_j \rangle}\right)}, \quad (7)$$

where $\Delta a_i, \Delta a_j$ are the energy resolution corrections per η bin defined by equation (6) and $\langle E_i \rangle, \langle E_j \rangle$ are the average electron energies per η bin.

3.3 Preparation of the data

3.3.1 Initial preparation

For the analysis presented in this report, 350 pb⁻¹ of data describing $J/\psi \rightarrow e^+e^-$ decays resulting from proton-proton collision was used. This has been collected by ATLAS at $\sqrt{s} = 13$ TeV between 2017 and 2018 and has $\langle \mu \rangle = 2$.

The events are required to pass the $J/\psi \rightarrow e^+e^-$ trigger chains optimised for the low $\langle \mu \rangle$ data set. The pre-selection criteria applied to individual electrons are: $p_T > 4.5$ GeV, $|\eta| < 2.47$ but $|\eta|$ outside the interval $[1.37, 1.52]$ due to bad reconstruction efficiency, and the fulfilment of the Medium likelihood-based identification criteria [6]. The pre-selection criteria applied to the dielectron system are: 2 electrons, $p_T > 5$ GeV for the leading electron and $p_T > 4.5$ GeV for the sub-leading one, and $2.1 < m_{ee} < 4.1$ GeV.

Additionally, the data has undergone an initial electron energy calibration using the decay $Z \rightarrow e^+e^-$ extrapolated into the appropriate energy range. In order to reduce background from misidentified electrons, a filter for electrons with opposite charge sign was applied.

3.3.2 Separation of prompt and non-prompt J/ψ

The J/ψ in which the dielectron system originates can be distinguished as either prompt, produced at the interaction point, or non-prompt, produced in secondary decays, such as the decay of a B^0 meson. The variable used to separate prompt and non-prompt J/ψ is the pseudoproper time τ , defined as:

$$\tau = \frac{L_{xy} m^{J/\psi}}{p_T^{J/\psi}}, \quad (8)$$

where L_{xy} is the decay length in the transverse plane defined as $L_{xy} = \mathbf{L} \cdot \mathbf{p}_{\mathbf{T}}^{J/\psi} / p_T^{J/\psi}$, where \mathbf{L} is the vector from the primary vertex to the J/ψ decay vertex and the remaining symbols have their usual meaning.

Since non-prompt J/ψ are produced further away from the interaction point, they have larger pseudoproper time. The data has been filtered to remove non-prompt J/ψ by excluding values of $\tau > 0.2$. The analysis presented in this report could however be carried for non-prompt J/ψ with minimal adjustments.

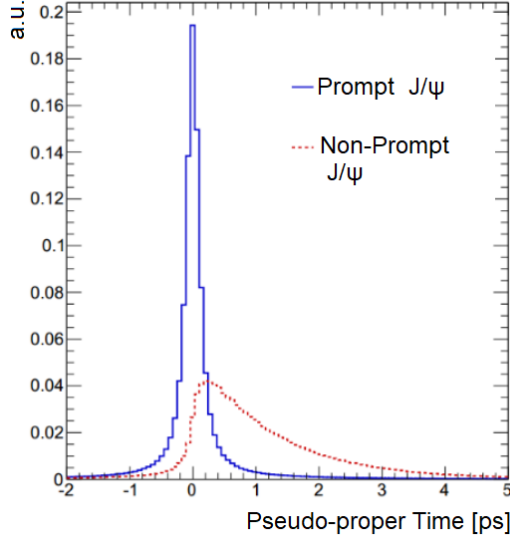


Figure 3: Monte Carlo simulation of the pseudoproper time distribution of prompt and non-prompt J/ψ [7].

3.4 Monte Carlo samples

Prompt J/ψ MC samples were generated and passed through a full Geant4 simulation of the ATLAS detector. The simulated prompt J/ψ samples are:

```
mc16_13TeV.P8B_A14_CTEQ6L1_Jpsie3e3.STDM6.e8461_e7400_s3126_r10244_r10210_p5243;
mc16_13TeV.P8B_A14_CTEQ6L1_Jpsie3e8.STDM6.e8461_e7400_s3126_r10244_r10210_p5243;
mc16_13TeV.P8B_A14_CTEQ6L1_Jpsie3e13.STDM6.e8461_e7400_s3126_r10244_r10210_p5243.
```

The samples were generated in slice of energy of leading and sub-leading electrons to cover the phase space of interest better. In order to combine the samples correctly, these are weighted according to the respective luminosity normalisation values. To check that the combination is correct, the distribution of p_T of the leading electron was plotted; this should be free of discontinuities.

From the evaluation of the p_T distribution, it was decided that a proper combination was not achieved. However, the combined MC was used in the analysis, making the work of this report a proof of concept for how the method works, acknowledging that the final results are not representative of the real energy scale corrections due to this fault in MC.

3.5 Fit of the data

The data is described using a signal and background probability distribution function (PDF). The J/ψ signal is modelled with a Double Sided Crystal Ball (DSCB) function

and the background has two components: a continuous irreducible background from Drell-Yan processes modelled with a 3rd order Chebychev polynomial and the $\psi(2s)$ resonance modelled with a DSCB function.

The standard method of fitting the data requires to first fit the J/ψ signal only from the MC and then to fix the parameters of the DSCB describing the signal in data to those resulting from MC. This allows for a better estimation of the background in the next steps of the fit. However, due to delays in obtaining the MC required for the presented project, an alternative was found for estimating the background without MC.

In order to remove the signal from background as much as possible, two additional filters were used on the data: fulfilment of the Tight likelihood-based identification criteria for individual electrons and electron $p_T > 5$ GeV. The background is still significant even with the added filters, so the PDF used still contained signal and background. The parameters obtained from this initial fit for the signal DSCB, Chebychev background and $\psi(2s)$ background were used as starting points for fitting the data again, but without the Tight and p_T filters.

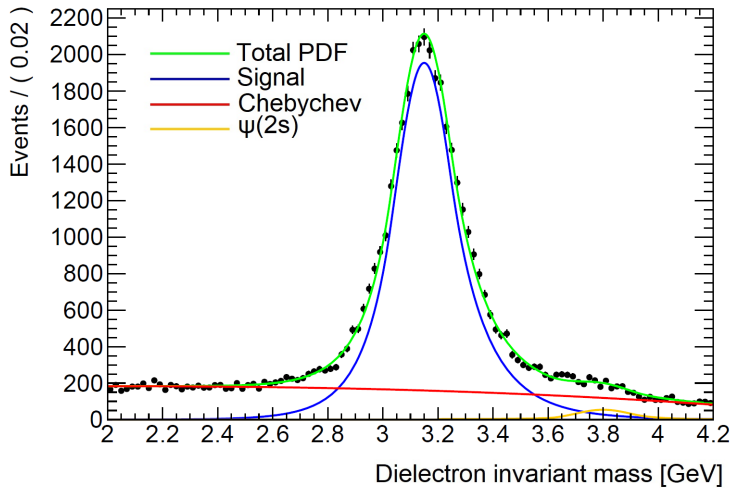


Figure 4: Fit of the data after filters for Tight electron identification criteria and $p_T > 5$ GeV were applied. With the background reduced, an enhanced fitting of the J/ψ signal was performed.

It is worth noting that the Chebychev shape was difficult to obtain because without a good constraint on the signal, the DSCB overestimates the tails. Additionally, the $\psi(2s)$ peak is difficult to model because of its closeness to the signal peak. Both of these aspects highlight the importance of the initial MC fit.

After this stage, the MC became available and in the final fit described in the next subsection, the α_{DSCB} and n_{DSCB} parameters of the signal DSCB were fixed to the ones obtained from MC. However, the background shape obtained through the method above

was found to be accurate enough, given that the reduced χ^2 value of the fit is $\chi^2 = 1.68$, and was kept in the final fit.

3.6 Data and Monte Carlo fit

In order to extract the energy scale correction and resolution from equations (5) and (7), a fit using both data and MC must be performed per regions of η . The measurement of the energy scale corrections was performed.

First, the signal in MC is fitted alone with a DSCB and then the data is fitted as such:

- the mean of the signal DSCB representing the J/ψ mass reconstructed in data is set according to formula (5). The mean of the MC DSCB is fixed to the value previously determined. The energy scale corrections α_i and α_j are left to float with starting value $\alpha_{i,j} = 0$ and $\alpha_{i,j} \in [-3, 3]$;
- the σ , α_{DSCB} and n_{DSCB} parameters of the signal DSCB are fixed to the values obtained in the initial MC fit;
- the three parameters of the Chebychev polynomial are fixed to the ones determined in the data only fit described in Subsection 3.5 to: $p_1 = -0.45$ (linear term), $p_2 = -0.1$ (quadratic term), $p_3 = -0.03$ (cubic term);
- the parameters of the $\psi(2s)$ DSCB are fixed to the ones determined in the data only fit described in Subsection 3.5 to: mean = 3.71, $\sigma = 0.1$, $\alpha_R = 0.8$, $n_R = 100$, $\alpha_L = 0.8$, $n_L = 100$.

Additionally, when adding the background PDFs a fractional weight f is added so that $\text{PDF}_{\text{Background}} = f * \text{PDF}_{\psi(2s)} + (1 - f) * \text{PDF}_{\text{Chebychev}}$ and f is left to float with starting value 0.07 and $f \in [0.01, 0.8]$. Similarly, the ratio of signal to total background PDF is f_{signal} defined so that $\text{PDF}_{\text{Total}} = f_{\text{signal}} * \text{PDF}_{J/\psi} + (1 - f) * \text{PDF}_{\text{Background}}$ and f_{signal} is left to float with starting value 0.5 and $f_{\text{signal}} \in [0.1, 0.9]$.

In order to obtain the energy resolution correction, the fit described above would be repeated by fixing the energy scale corrections α and replacing the σ parameter of the signal DSCB in data according to equation (7), with $\sigma_{m_{ee}^{MC}}$ fixed from the initial MC fit.

4 Results

An illustrative fit of the data in a given η region is shown in Figure 5. Out of 36 η regions resulting from the binning described in Section 2.2, 23 of them were excluded due to low numbers of events. This could be due to the fact that J/ψ is boosted so the two resulting electrons are close in η . An improvement in the analysis would be to bin the data according to $|\eta|$ in order to increase the number of events per given $|\eta|$ region.

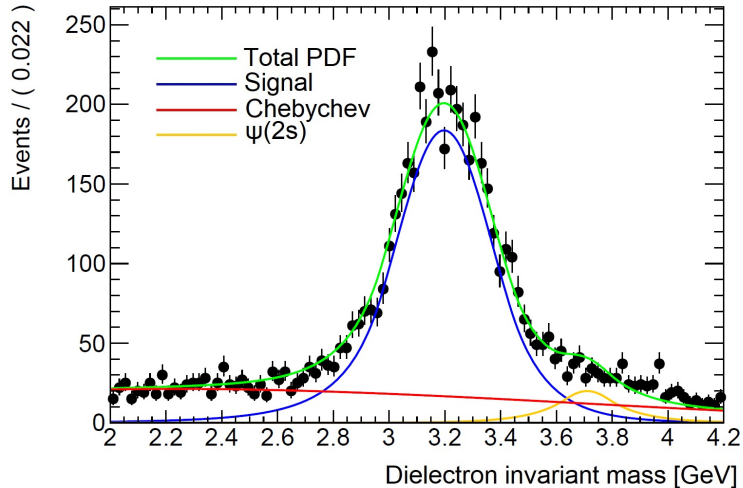


Figure 5: Fit of the data with the background fixed from the method described in Section 3.5 and the signal modelled using parameters fixed by the Monte Carlo simulation as described in Section 3.6. The pseudorapidity region corresponding to this plot is $-0.8 < \eta_{e1} < -0.4$ and $-1.37 < \eta_{e2} < -0.8$.

The values for the energy scale correction per pseudorapidity region $\alpha(\eta)$ are presented in Table 1. As described in Subsection 3.4, due to delays in the production of the MC customised for the very low pile-up regime, the combination of MC samples cannot be properly used, so the results serve only as proof that the method can be used to constrain the energy scale corrections.

Due to time considerations, the determination of energy resolution corrections Δa and thus of the effective sampling term a was not pursued in the project, although its implementation in the existing framework is straightforward, as argued at the end of Section 3.6.

Table 1: Values of the energy scale correction α per η regions

α	Error in α	$\eta \in [\eta_{\text{low}}, \eta_{\text{high}}]$
5.3×10^{-3}	8×10^{-4}	$[-2.47, -1.52]$
1.3×10^{-2}	1×10^{-3}	$[-1.37, -0.8]$
4.6×10^{-3}	8×10^{-4}	$[-0.8, -0.4]$
4.3×10^{-3}	7×10^{-4}	$[-0.4, 0]$
3.9×10^{-3}	7×10^{-4}	$[0, 0.4]$
4.5×10^{-3}	7×10^{-4}	$[0.4, 0.8]$
1.3×10^{-2}	1×10^{-3}	$[0.8, 1.37]$
2.3×10^{-3}	8×10^{-4}	$[1.52, 2.47]$

5 Conclusion and discussion

A method to determine the effective sampling term a from the relative energy resolution of electrons detected with the ATLAS Liquid Argon Calorimeter was presented and the determination of the energy scale correction per regions of pseudorapidity was pursued. This is achieved by comparing the J/ψ mass resonance peak between data and the Monte Carlo simulation, using 350 pb^{-1} of low pile-up data.

Due to delays in the production of the MC, an alternative method for estimating the background from data was found, leading to insights into the interplay between continuous and resonant background around the J/ψ mass.

Although the determination of the energy resolution correction was not possible due to time constraints, its implementation in the existing framework is straightforward and could be the subject of future work. The inclusion of non-prompt J/ψ could also be a future addition to the analysis presented.

The improved method to determine the effective sampling term, a , described in this report translates into better modelling of the response of the ATLAS LAr Calorimeter in new energy and pile-up regimes. Thus, the results of this report are relevant to the various precision measurements and searches carried with the ATLAS detector.

References

- [1] G. Aad et al. The ATLAS Experiment at the CERN Large Hadron Collider. *JINST*, 3:S08003, 2008.
- [2] Joao Pequeno. Computer generated image of the ATLAS Liquid Argon. 2008.
- [3] G Unal. Electron and Photon energy resolutions and their uncertainties for run-1 calibration. Technical report, CERN, Geneva, 2013.
- [4] Georges Aad et al. Electron and photon performance measurements with the ATLAS detector using the 2015–2017 LHC proton-proton collision data. *JINST*, 14(12):P12006, 2019.
- [5] Knut Zoch. *Cross-section measurements of top-quark pair production in association with a hard photon at 13 TeV with the ATLAS detector*. PhD thesis, Gottingen U., 2020.
- [6] Morad Aaboud et al. Electron reconstruction and identification in the ATLAS experiment using the 2015 and 2016 LHC proton-proton collision data at $\sqrt{s} = 13$ TeV. *Eur. Phys. J. C*, 79(8):639, 2019.
- [7] Andrey Kupich. Electron ID efficiency measurements with J/ψ TP τ -cut framework.